Theoretical Prediction of EPR Coupling Constants for the Determination of the Selectivity in the OH Addition to Toluene

Victor Hugo Uc,[†] Isidoro García-Cruz,[‡] André Grand,[§] and Annik Vivier-Bunge*,[‡]

Departamento de Química, Universidad Autónoma Metropolitana, Iztapalapa, 09340 México, D.F., México. Programa de Simulación Molecular, Instituto Mexicano del Petróleo, 07730 México, D.F. México, and Département de Recherche Fondamentale sur la Matière Condensée, CEA-Grenoble, 17 Rue des Martyrs, 38054 Grenoble Cedex 9, France

Received: January 4, 2001; In Final Form: April 12, 2001

High-level theoretical methods based on density functional and Hartree−Fock−Møller−Plesset theories have been employed to study the selectivity of the OH radical attack on toluene and to predict expected hyperfine coupling constants of the isomeric addition adducts. In recent work, we have found that the adduct with $OH^\bullet$ added to the methyl-substituted carbon atom (ipso addition) of the ring may be especially stable both in toluene and in the xylenes. However, since this kind of adduct does not form a phenol, it is not directly identified in the products. The calculations indicate that quite different values should be observed for the EPR signals of the methyl hydrogen atoms of the four isomers, suggesting that electron paramagnetic resonance measurements could provide decisive information on the selectivity of the $OH^\bullet$ addition to toluene. The calculated values of the hyperfine coupling constants are compared with the experimental values reported by Jolibois et al. for thymine.

1. Introduction

It is well-known that the initial reaction of toluene in the troposphere involves, almost exclusively, the $OH^\bullet$ radical,[1] via two possible pathways: the abstraction of a hydrogen atom from the side chain to form a benzyl radical and water,

$$Ar-CH_3 + OH^\bullet \rightarrow Ar-CH_2^\bullet + H_2O \qquad (1)$$

and the addition of the $OH^\bullet$ radical to the ring,

$$Ar-CH_3 + OH^\bullet \rightarrow Ar(OH)-CH_3^\bullet \qquad (2)$$

For reaction 2, several $OH^\bullet$ addition isomers are expected to be formed. In toluene, $OH^\bullet$ can in principle add to the ortho, meta, or para positions, and also to the carbon atom to which the methyl group is attached (ipso position).

The adducts formed in the addition reaction have not been isolated. Only in the case of benzene has the OH adduct been observed in the gas phase using UV absorption at 308 nm.[2] Their existence is postulated on the basis of part of the observed final products: *o*-, *m*-, and *p*-cresols and *o*-, *m*-, and *p*-nitrotoluene. Since no cresol can be obtained from addition at the ipso position, the possibility of this adduct being formed has not been considered, in general.

The kinetics and mechanisms of the OH radical reaction with toluene has been reviewed and evaluated by Atkinson.[3] For toluene at 298 K, approximately 10% of the overall reaction occurs by H atom abstraction to form, in the presence of NO, benzaldehyde and benzyl nitrate. The cresols account for approximately 25% of the overall OH radical reaction, and glyoxal plus methylglyoxal (together with their coproducts) for another 25%. The remaining 40% reaction products are not quantitatively known, although a variety of ring cleavage products (other than the already mentioned α-dicarbonyls) have been observed. Thus, considerable uncertainty still exists regarding the overall $OH^\bullet$ + toluene reaction.

According to the accepted rules for electrophilic addition to aromatic rings, one would expect addition to occur at the ortho and para position. However, the observed preference for attack at the ortho position of toluene by a factor of 5.6 with respect to the para position is significantly greater than the statistical preference of a factor of 2.

Theoretical work on the oxidation reactions of aromatic hydrocarbons is scarce. Bartolotti and Edney[4] used a simple density functional approach with the local exchange correlation functional developed by Vosko−Wilk−Nusair[5] to identify potential intermediates produced in the $OH^\bullet$ addition initiated atmospheric photooxidation of toluene. Although their energy results were acknowledgably preliminary in nature, their calculations were able to confirm certain aspects of the proposed reaction mechanism[3] and to predict the importance of carbonyl compounds containing epoxide structures. More recently, Andino et al.[6] performed very extensive and complete theoretical work on the atmospheric oxidation of toluene, *m*- and *p*-xylenes, 1,2,4-trimethylbenzene, and *m*-ethyltoluene. These authors used a combination of semiempirical (PM3) and density functional theory (using the hybrid B3LYP functional[7]) to calculate the energies and structures of all the postulated intermediates and products along several possible pathways, up to the final products. In both of these papers[4,6] only the pathways following the $OH^\bullet$ addition at the ortho position were considered.

In previous work on the selectivity of $OH^\bullet$ addition to toluene[8,9] and to xylenes[10] using second-order Møller−Plesset perturbation theory (MP2) and B3LYP calculations, we found a significant contribution from adducts corresponding to addition of the OH radical to the ipso carbon atom. The possibility of addition at this position, however, has not been considered in general, except for *o*-xylene, and the various proposed mechanisms do not mention channels arising from the ipso adducts.

[†] Universidad Autónoma Metropolitana.
[‡] Instituto Mexicano del Petróleo.
[§] CEA-Grenoble.

10.1021/jp0100405 CCC: $20.00

For *o*-xylene several authors[11,13,14] propose schemes involving addition of OH$^\bullet$ to an ipso carbon atom, to explain the observed ring cleavage final products and the formation of biacetyl.[11] Yet, as discussed by Traynham,[12] numerous examples of ipso free-radical substitution have been reported.

We have recently calculated the potential energy surface for the initial OH$^\bullet$ attack on toluene, including the formation of a pre-reactive complex that explains the observed negative activation energies in reaction 2.[9] A discrepancy was observed between the results obtained using a B3LYP density functional approach, on one hand, and either Hartree−Fock−Møller−Plesset (MPn) or coupled cluster (CC) theories, on the other hand, with respect to the importance of the ipso OH$^\bullet$ addition. Although MPn and CC results indicated that addition at this position of the ring yielded adducts that were especially stable both in toluene and in the xylenes, B3LYP calculations systematically deemphasized those interactions that should be responsible for their added stability. However, even considering the possibility that the stability of the ipso derivative could be exaggerated in the MPn and CC calculations, the formation of this adduct is certainly not negligible, and it should yield detectable concentrations of certain products, as observed in the case of the meta and para isomers. In ref 9, three schemes were proposed for the fate of the ipso adduct.

Because the adducts are free radicals, electron paramagnetic resonance spectroscopy (EPR) should be the appropriate type of spectroscopy to characterize the isomers and to determine the selectivity. Indeed, both experimental and theoretical[15] results are available for a few similar compounds, i.e., the OH$^\bullet$ and H$^\bullet$ addition adducts of DNA bases. In the present work, the hyperfine coupling constants of specific atoms in the different isomeric addition adducts will be calculated, to determine whether they could eventually be used to experimentally identify the different isomers.

2. Computational Methodology

Electronic structure calculations have been performed with the system of programs Gaussian98 (G98).[16] Restricted Hartree−Fock theory (RHF) was used for closed-shell systems, and unrestricted Hartree−Fock theory (UHF) for open-shell systems (radicals). All geometries were fully optimized at the MP2 and B3LYP levels using a 6-31G** basis set. Spin densities were obtained using Møller−Plesset perturbation theory up to second order (MP2), with density functional theory using the B3LYP hybrid functional[7] and with the singles and doubles coupled cluster method CCSD, using several basis sets. Projected MP2 energies (PMP2) were used throughout in order to correct for spin contamination. Single-point B3LYP calculations were performed with the EPR-II basis set, which was specifically optimized to yield improved magnetic properties when used with the B3LYP method.[17,18] EPR-II is a double-ζ basis set with a single set of polarization functions and an enhanced *s* part designed to describe better the nuclear region.

Hyperfine coupling constants are related to the spin densities at the corresponding nuclei by the following equation:

$$a_{\mathrm{N}} = \frac{8\pi}{3h} g_{\mathrm{e}} \beta_{\mathrm{e}} g_N \beta_N \sum_{\mu,\nu} P_{\mu,\nu}^{\alpha-\beta} \langle \phi_\mu | \delta(r_{kN}) | \phi_\nu \rangle \qquad (3)$$

where g_e is the free electron *g*-factor and *h* is the Planck constant. The sum in the previous equation is the spin density directly given in Gaussian 98. In the present work, all the values are given in Gauss (1 G = 0.1 mT), assuming that the free electron *g* value is appropriate also for the radicals. To convert data to megahertz, one has to multiply them by 2.8025.

Averaging of the hyperfine coupling constants of the three hydrogen atoms in the methyl group is in order if there is a free rotation about the C−CH$_3$ bond. In this work, the energy barriers for this rotation were computed for the four isomers. In addition, other large amplitude vibrations capable of affecting the EPR coupling constants were analyzed.

3. Results and Discussion

Our present study investigates the addition products in the initial reaction of a hydroxyl radical with toluene. We consider the four isomers of the adducts of toluene. Their geometries were obtained at the MP2/6-31G** and B3LYP/6-31G**, and the MP2-optimized structures are shown in Figure 1, including the numbering of the atoms. All the parameters are given in Table 1 for the ipso adduct, for the two methods employed. Corresponding tables for the other isomers are available as Supporting Information. As expected for stable structures in general, most distances and angles for the two methods are very similar. Differences in the values of the distances are typically less than 0.01 Å, those of the angles fall within less than 1°, and those of dihedral angles within 2°. However, it is interesting to note that, for all the isomers, one of the C−C bonds is considerably longer (0.025 Å) in the B3LYP geometry than in the MP2 one. These bonds are indicated in boldface in the tables. They happen to be, in all cases, those that occupy an α position with respect to the carbon atom carrying the largest spin density. The disagreement is probably due to the fact that the two methods differ appreciably in their description of the radical center. In fact, MP2 tends to better localize the spin density, and thus the corresponding bond distance is shorter.

The relative PMP2 and B3LYP energies, including the zero point energy corrections (ZPE), calculated with respect to the energy of the ortho adduct, are given in Table 5. Calculations using perturbation theory agree that the isomer with OH$^\bullet$ attached to the ipso carbon atom is slightly more stable than the ortho isomer. The density functional method, instead, favors the ortho OH$^\bullet$ isomer. In particular, the interactions between the oxygen atom and the methyl group in ipso additions are given very little weight in calculations with B3LYP, since the para isomer is the second most stable adduct, and it is only 0.86 kcal/mol less stable than the ortho isomer. In the MP2 calculations, two specific interactions appear to be responsible for the extra stability of the ipso isomer: (i) the interaction between the oxygen atom and the carbon atom of the methyl group, the O$\cdots$C distance being about 2.35 Å; and (ii) the interaction between the lone pairs on the oxygen atom and two hydrogen atoms of the methyl group, the distance between these atoms being about 2.57 Å.

Discrepancies between MP2 and B3LYP results have also been observed in other systems,[10] with B3LYP systematically deemphasizing the interactions responsible for the extra stability of the ipso adducts.[9] It is interesting to compare these results with those obtained by Jolibois et al.[19] for the OH$^\bullet$ addition to the thymine molecule. In this case, B3LYP calculations indicate a slight preference for the ortho adduct (addition at C6), while according to direct experimental results[20] approximately 60% of the products correspond to ipso addition (C5), 35% occur at the ortho position, and 5% correspond to hydrogen abstraction from the methyl group.

The MP2/6-31G** ZPE corrections for position isomers are found to be about 91.5, 91.2, 91.3, and 91.3 kcal/mol for the ortho, ipso, meta, and para adducts respectively, while the

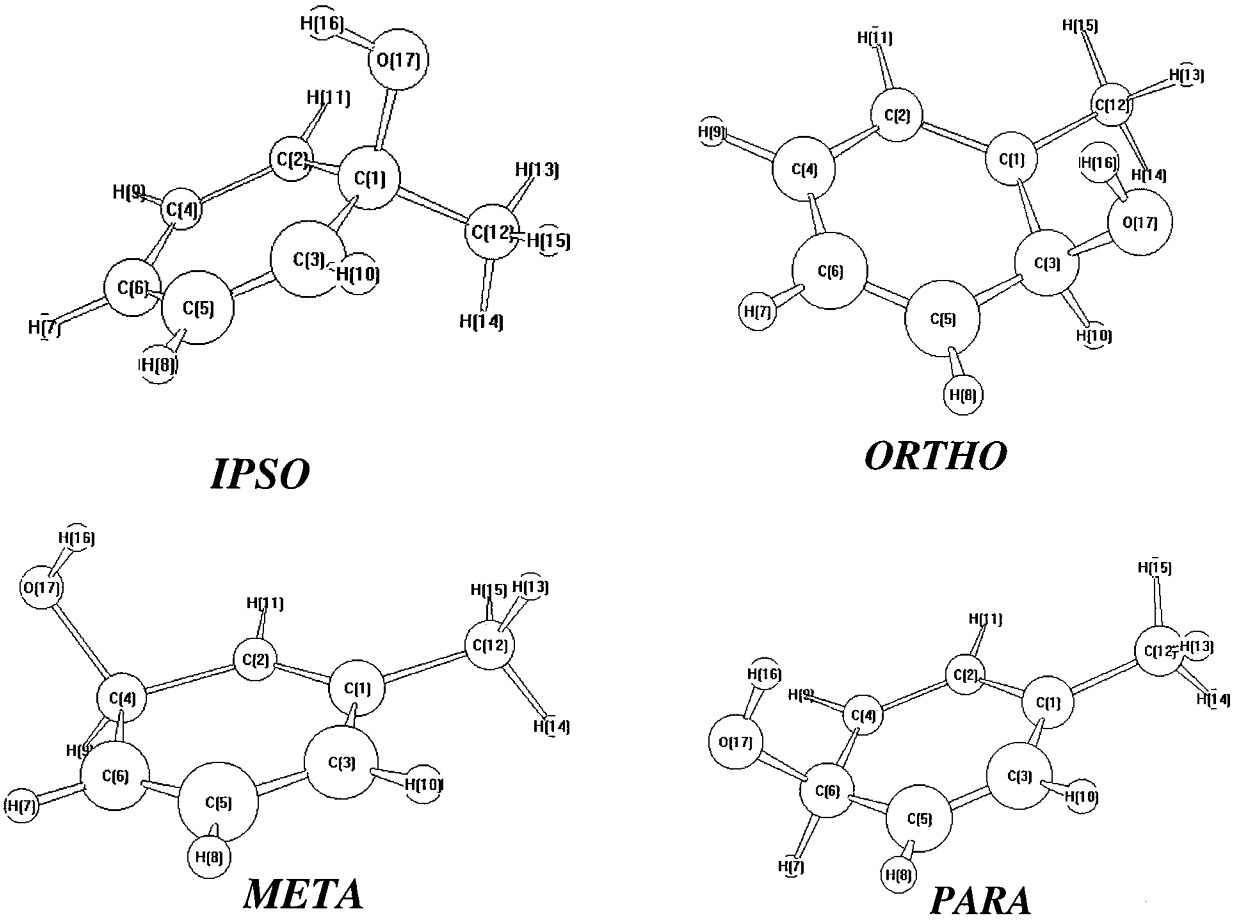

Figure 1. MP2-optimized geometries of the OH adducts.

TABLE 1: MP2/6-31G and B3LYP/6-31G** Geometrical Parameters of the Ipso OH−Toluene Adduct**

parameter	MP2	B3LYP	parameter	MP2	B3LYP	parameter	MP2	B3LYP
$r(\mathrm{C_1C_2})$	1.5002	1.5080	$A(C_3C_1C_2)$	111.999	111.912	$D(C_4C_2C_1C_{12})$	122.895	123.734
$\mathbf{r(C_2C_4)}$	**1.3434**	**1.3668**	$A(C_1C_2C_4)$	123.165	123.062	$D(C_2C_1C_{12}H_{13})$	57.989	57.981
$r(C_4C_6)$	1.4180	1.4185	$A(C_2C_4C_6)$	121.109	121.154	$D(C_2C_1C_{12}H_{14})$	-62.505	-62.568
$r(C_1C_{12})$	1.5276	1.5387	$A(C_4C_6C_5)$	119.404	119.637	$D(C_4C_2C_1O_{17})$	-123.044	-122.389
$r(C_2H_{11})$	1.0830	1.0870	$A(C_2C_1C_{12})$	110.837	111.000	$D(C_2C_1O_{17}H_{16})$	61.553	61.489
$r(C_4H_9)$	1.0826	1.0871	$A(C_1C_2H_{11})$	115.610	115.892			
$r(C_6H_7)$	1.0799	1.0850	$A(C_2C_4H_9)$	119.929	119.696			
$r(C_{12}H_{13})$	1.0895	1.0942	$A(C_4C_6H_7)$	120.282	120.175			
$r(C_{12}H_{14})$	1.0881	1.0928	$A(C_1C_{12}H_{13})$	109.428	109.683			
$r(O_{17}H_{16})$	0.9675	0.9680	$A(C_1C_{12}H_{14})$	110.365	110.880			
$r(C_1O_{17})$	1.4501	1.4551	$A(C_{12}C_1O_{17})$	103.933	103.712			
			$A(C_1O_{17}H_{16})$	105.654	106.409			

TABLE 2: Summary of MP2/6-31G and B3LYP/6-31G** Total Energies, S^2 Values before and after Projection, and Thermodynamical Data for the OH−Toluene Isomers**[a]

	ipso		ortho		meta		para	
	MP2	B3LYP	MP2	B3LYP	MP2	B3LYP	MP2	B3LYP
total E (hartrees)	−346.257 167	−347.338 283	−346.256 185	−347.340 582	−346.253 164	−347.337 878	−346.253 540	−347.338 860
ZPE (hartrees)	0.145 386	0.141 414	0.145 793	0.141 719	0.145 487	0.141 437	0.145 561	0.141 360
S^2								
before	1.1401	0.789	1.137	0.788	1.134	0.766	1.138	0.765
after projection	0.8472	0.751	0.8460	0.751	0.8450	0.750	0.8470	0.750
E_{rel} (kcal)	−0.92	1.64	0.	0.	2.10	1.80	1.86	0.86
S_{298} (cal/K)	84.7	85.2	86.0	86.5	86.7	87.2	89.1	91.2
G_{rel} (kcal)	−0.44	1.63	0.	0.	1.17	1.02	−0.11	−1.80

[a] E_{rel} is the total energy and G_{rel} is the Gibbs free energy at 298 K, per mole, relative to those of the ortho isomer.

corresponding B3LYP/6-31G** values are 88.9, 88.7, 88.7, and 88.7 kcal/mol. Trends are the same with the two methods, with the ortho ZPE correction being the largest. A summary of calculated thermodynamic data is given in Table 2. The entropy is smallest for the ipso, and largest for the para isomer, in the two methods. With MP2, both the total energy and the Gibbs free energy favor the formation of the ipso isomer. Moreover, both methods yield Gibbs free energy results that are more negative for the para isomer than for the ortho isomer. It is interesting to discuss the possible implications of this result.

TABLE 3: Spin Densities on the Atoms of the Ipso OH−Toluene Radical

	MP2/6-31G**	CCSD/6-31G**// MP2/6-31G**	B3LYP/ 6-31G**	B3LYP/EPRII// B3LYP/6-31G**
1 C	−0.0224	−0.0505	−0.0592	−0.0427
2 C	0.3391	0.4268	0.4387	0.4200
3 C	0.3391	0.4268	0.4387	0.4200
4 C	−0.1493	−0.2546	−0.2190	−0.1865
5 C	−0.1493	−0.2546	−0.2190	−0.1865
6 C	0.6375	0.6977	0.5747	0.5382
7 H	−0.0313	−0.0323	−0.0267	−0.0301
8 H	−0.0063	−0.0001	0.0076	0.0094
9 H	−0.0063	−0.0001	0.0076	0.0094
10 H	−0.0106	−0.0150	−0.0202	−0.0230
11 H	−0.0106	−0.0150	−0.0202	−0.0230
12 C	0.0200	0.0214	0.0305	0.0375
13 H	0.0040	0.0036	0.0045	0.0031
14 H	0.0001	−0.0001	−0.0006	−0.0010
15 H	0.0040	0.0038	0.0045	0.0031
16 H	0.0082	0.0065	0.0081	−0.0008
17 O	0.0339	0.0359	0.0501	0.0530

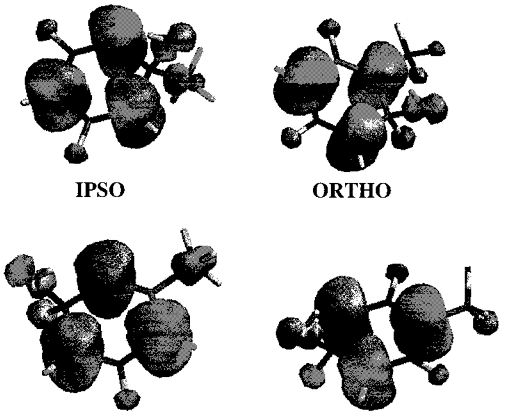
IPSO ORTHO

META PARA

Figure 2. Positive spin densities of the OH adducts.

Considering that experiments indicate an observed preference for attack at the ortho position of toluene by a factor of almost 6 with respect to the para position, we have suggested[9] that the ipso adduct may undergo a 1,2 OH shift, to form more ortho adduct.

Also given in Table 2 are the $\langle S^2 \rangle$ values before and after projection of higher spin states. It is seen that contamination by spin states corresponding to quartets and sextets is especially important with the MP2 method but that most of it is eliminated by projection. The B3LYP method does not have this problem.

Table 3 contains the spin density results obtained with different methods of calculation and different basis sets, for the ipso isomer. Corresponding tables for the other isomers are available as Supporting Information. As expected, large differences are observed between the columns in these tables. Indeed, it is well-known that charge and spin densities may vary widely from one method to the other. Trends, however, agree reasonably. The results obtained with the coupled cluster method are the ones that differ most. Indeed, when this method is used, spin contamination is about the same as in MPn, but formulas to project out the terms correpsonding to higher spin states are not available. Thus, as observed in other cases,[21,22] the CC method does not yield good results when spin contamination is considerable.

In Figure 2, the B3LYP/EPRII positive spin densities of the four adduct isomeric species have been represented. It can be seen that, in all the isomers, there is a large spin polarization on the aromatic cycle. The characteristic alternance of large positive and negative spin densities on the carbon atoms indicates that the radical electron is quite delocalized over the atoms of the ring. This behavior contrasts with the one observed in the case of two OH−thymine isomers (Figure 3),[19] where the radical electron is mainly localized on the carbon atom adjacent to the addition site. In all the OH−toluene isomers, the largest positive spin density is localized on the carbon atom opposite to the one to which OH is attached.

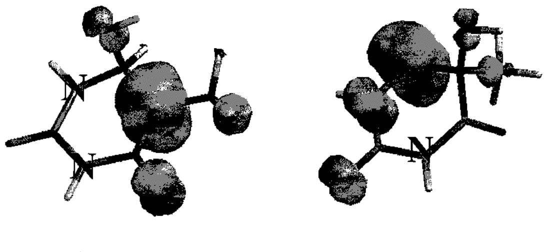
ORTHO IPSO

Figure 3. Positive spin densities of *ipso*- and *ortho*-OH−thymine.

TABLE 4: Fermi Contact Term on the Atoms of the Ipso OH−Toluene Radical

	MP2/6-31G**	CCSD/6-31G**// MP2/6-31G**	B3LYP/ 6-31G**	B3LYP/EPRII// B3LYP/6-31G**
1 C	−0.0009	−0.0107	−0.0205	−0.0257
2 C	0.0144	0.0324	0.0468	0.0354
3 C	0.0144	0.0324	0.0468	0.0354
4 C	−0.0039	−0.0234	−0.0332	−0.0349
5 C	−0.0039	−0.0234	−0.0332	−0.0349
6 C	0.0568	0.0714	0.0619	0.0455
7 H	−0.0091	−0.0098	−0.0086	−0.0084
8 H	−0.0030	−0.0007	0.0024	0.0027
9 H	−0.0030	−0.0007	0.0024	0.0027
10 H	−0.0025	−0.0042	−0.0065	−0.0066
11 H	−0.0025	−0.0042	−0.0065	−0.0066
12 C	0.0349	0.0350	0.0404	0.0466
13 H	0.0010	0.0010	0.0012	0.0012
14 H	0.0007	0.0006	0.0007	0.0006
15 H	0.0010	0.0010	0.0012	0.0012
16 H	−0.0008	−0.0009	−0.0013	−0.0016
17 O	0.0347	0.0345	0.0384	0.0486

The Fermi contact terms of the ipso adduct, obtained with four different methods and basis sets, are given in Table 4. The corresponding tables for the other isomers are available as Supporting Information. Some systematic results are observed:

(i) For all the hydrogen atoms attached to carbon atoms carrying the largest positive spin densities, the Fermi contact terms are very similar, about 0.008.

(ii) For all the hydrogen atoms attached to carbon atoms adjacent to the addition site, the Fermi contact terms are about 0.006.

We are especially interested in the Fermi contact terms of the methyl hydrogen atoms because they differ substantially from one isomer to the other, suggesting that they might be used to determine the selectivity. Analogously, large variations are observed in the Fermi contact terms of the methyl carbon atom in the different isomers. Instead, the OH hydrogen atom and those attached to the ring carbon atoms present very similar spin densities in all isomers.

As discussed by Barone et al.,[18] averaging of the hyperfine coupling constants over large amplitude vibrational motions can sometimes be significant. In addition to the methyl torsion, another large amplitude motion, occurring at a frequency of about 80 cm^{-1}, corresponds to an equatorial-axial inversion at the addition site. Fortunately, in the case of the toluene isomers, the equilibrium form corresponds to the planar ring, so that this vibration should have a negligible effect on the experimental

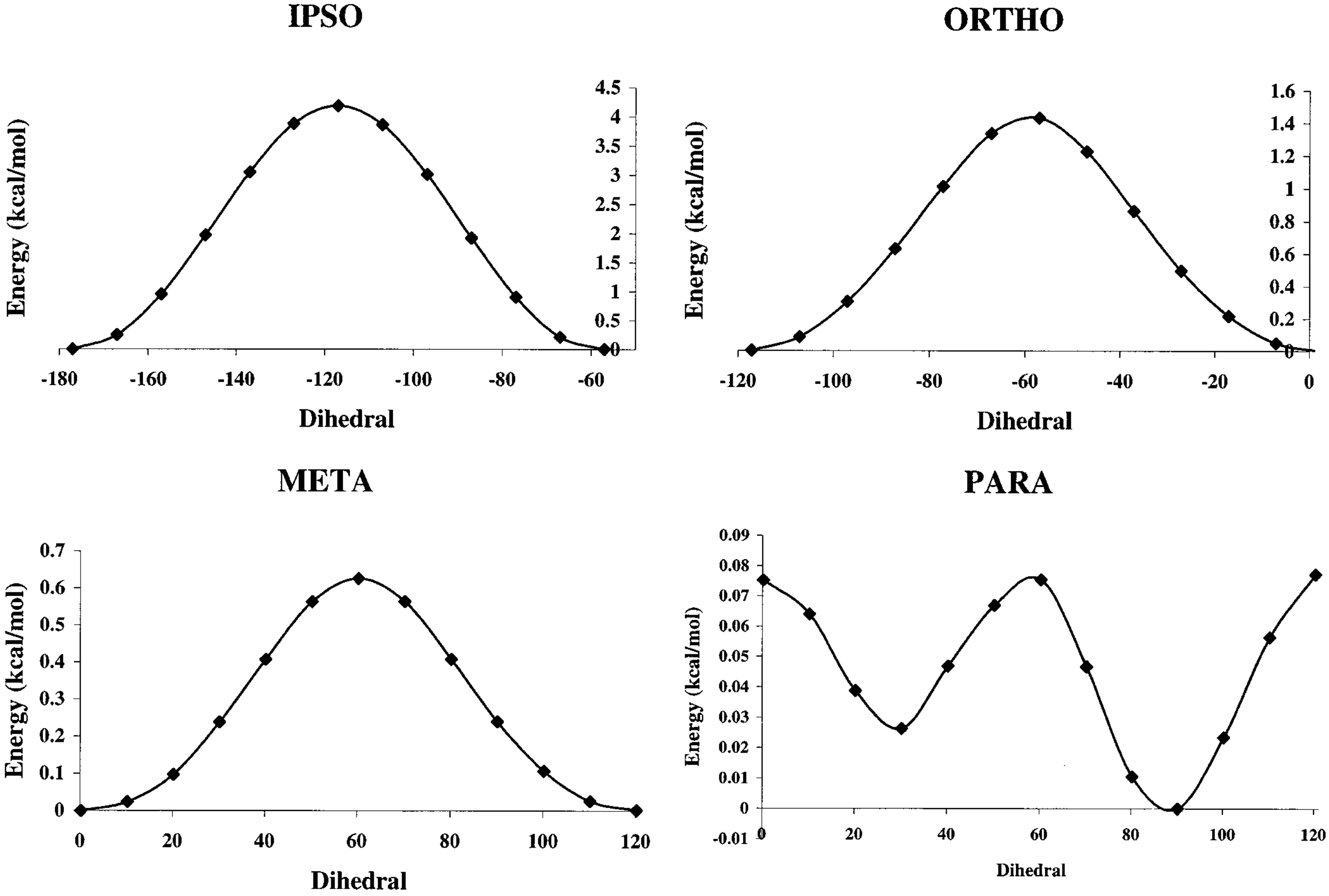

Figure 4. MP2/6-31G** total energies of the OH−toluene isomers as a function of the methyl torsion angle.

EPR results. For comparison, in the case of thymine, an asymmetric double minimum potential was obtained for this vibration, one of the equilibrium positions being much more stable than the other, so that proper account of vibrational modulation effects had to be made[15] by using an effective large amplitude nuclear Hamiltonian.

The B3LYP/EPRII calculated hyperfine coupling constants (hcc) are given in Table 5. It is interesting to discuss in detail the following points:

(1) Methyl Hydrogen Atoms. The hcc's are always the same for two of the methyl hydrogen atoms, while the third is entirely different, reflecting the fact that, in the equilibrium conformation, one hydrogen atom is approximately axial and the other two are much closer to the aromatic plane. However, rotation of the methyl group in the OH−toluene isomers may lead to the observing of only one coupling constant, corresponding to the arithmetic average of the values for the three hydrogen atoms involved. To verify this point, the total energy of the four adducts was calculated as a function of the methyl torsion angle. Plots are given in Figure 4. As expected, the largest rotation barrier corresponds to the ipso isomer (4.2 kcal/mol). The ones for the other isomers are much smaller. A double minimum is observed in the case of the para isomer, but barriers are less than 0.05 kcal/mol. Assuming that the rotation is approximately free, and that the three hydrogen atoms are equivalent, one obtains an hcc of +1.65, +10.88, −3.87, and +15.5 G, for the ipso, ortho, meta, and para isomers, respectively. On the basis of these mean values, it is obvious that the ipso isomer should be detected unambiguously. The para and ortho isomers could be separated also. The case of the meta isomer is somewhat different: its hcc is weak, as for the ipso adduct, but its sign is opposite. In addition, the thermodynamic preferences indicate that it should not exist in appreciable quantities.

TABLE 5: Hyperfine Coupling Constants in Gauss, Calculated at the B3LYP/EPRII Level Using the B3LYP/6-31G-Optimized Geometries, for the Four OH−Toluene Adducts**

atom	ipso	ortho	meta	para
1 C	−10.32	15.20	−14.14	19.60
2 C	14.22	−14.18	13.84	−14.03
3 C	14.22	−11.09	18.89	−14.03
4 C	−14.02	17.97	−11.27	14.11
5 C	−14.02	13.68	−14.50	14.11
6 C	18.25	−13.73	15.07	−11.07
7 H	−13.47	4.18	−10.92	39.86
8 H	4.31	−10.19	4.51	−10.24
9 H	4.31	−13.31	41.63	−10.24
10 H	−10.51	36.21	−13.77	4.20
11 H	−10.51	4.41	−9.87	4.20
12 C	18.69	−5.48	2.22	−7.70
13 H	1.97	15.63	−5.36	7.93
14 H	1.02	16.46	−5.47	30.66
15 H	1.97	0.55	−0.77	7.93
16 H	−2.52	−2.08	−1.96	−1.98
17 O	−10.52	−14.08	−14.96	−15.60

The above features lead to the conclusion that the methyl hydrogen atoms are good candidates for the detection of the presence of the ipso isomer.

(2) Methyl Carbon Atom. The data in Table 5 show that the hcc of this extracyclic carbon atom is also a good probe to determine the presence of the ipso isomer. Its hcc in the ipso isomer is calculated to be 18.69 G, much larger than the one for any of the other isomers (−5.48, +2.22, and −7.70 for the ortho, meta, and para forms, respectively). This is especially

TABLE 6: Predicted Hyperfine Coupling Constants in Gauss of Relevant Atoms, for the OH−Toluene Isomers[a]

					thymine			
	toluene				ipso		ortho	
atom	ipso	ortho	meta	para	calc	exp	calc	exp
methyl ^{1}H	1.65	10.88	−3.87	15.51	1.4	weak	20.7	22.3 (23.6)
methyl ^{13}C	18.69	−5.48	2.22	−7.70	18.4		−9.5	
^{17}O	−10.52	−14.08	−14.96	−15.60	−3.6		−17.69	
^{1}H at addition site		36.2	41.6	39.8			8.4	15.1 (10.8)

[a] The available experimental and calculated corresponding values for thymine are given for comparison.

noteworthy because it should be the easiest position to be replaced by a ^{13}C isotope. We can add that the other isomers could also be differentiated if the signs of the hcc's were determined, which requires an additional experimental effort. Thus, the methyl carbon constitutes a possible signature of the ipso isomer.

(3) Oxygen Atom. The hcc's of the ^{17}O atom can also be used to prove the ipso isomer's presence. Its hcc of −10.52 G differs very much from the ones in the other three isomers, which are all close to −14 G. The replacement of ^{16}O by ^{17}O in this molecule should be feasible. It is interesting to note that, although the absolute values are different, the trends are the same as those observed in the OH ipso and ortho derivatives of thymine,[19] the ipso hcc being weaker than the ortho.

(4) Hydrogen Atom at the Addition Site. Indeed, this ^{1}H hcc is of primary importance for our purpose. As can be seen from Table 5, in all cases, its hcc is about 30 G. Since there is no hydrogen atom at the addition site in the ipso isomer, this strong coupling should not be observed for this isomer. If no hcc is found in this range, it could be a definitive proof for the existence of the ipso isomer.

In Table 6, the predicted EPR coupling constants for the four isomers are given. The results are compared, when possible, with those observed in thymine,[15] because it is one of the few cases for which experimental results are available (refs 23 and 24 for the OH radical added at positions ipso and ortho, respectively, with respect to the methyl group in thymine) and they agree with the calculated values. The comparison of the two OH adducts of thymine indicates that both thymine and toluene adducts present a similar behavior. General trends are the same, even if absolute values differ considerably. These differences, however, are easily explained by the fact that the half-chair conformation at the addition site is much more pronounced in thymine than in toluene.

4. Conclusions

In this paper and in a previous one,[9] we have studied the thermodynamical stability of the ipso isomer of the OH adduct of toluene and we have shown that it is certainly formed in a significant ratio with respect to the other isomers. Because this adduct does not give a cresol product, however, it is not ordinarily taken into account in the reaction mechanisms proposed for toluene oxidation. In the present work we propose a spectroscopic investigation of this OH$^\bullet$ addition product, using electron paramagnetic resonance. We show that, under the correct conditions, it should be possible to prove the formation of the ipso adduct on the basis of its spectroscopic EPR properties. Four specific hyperfine coupling constants are described, which could lead to detection of the ipso isomer. In this isomer:

(i) the methyl hydrogen atoms have an especially low hcc,

(ii) the ^{13}C methyl carbon atom has the largest hcc,

(iii) the ^{17}O has the smallest hcc, and

(iv) the ^{1}H atom at the addition site is absent altogether while it has a very large hcc in the other isomers.

We believe that EPR experiments could thus prove unambiguously the importance of OH$^\bullet$ ipso addition to toluene, and also to aromatic rings in general.

Acknowledgment. We gratefully acknowledge the financial support from the Instituto Mexicano del Petróleo through program FIES-95-97-VI and from the CEA, Grenoble, for computing time.

Supporting Information Available: Tables of geometrical parameters, spin densities on all atoms, and Fermi contact terms on all atoms, of the ipso, ortho, meta, and para OH−toluene adducts. This material is available free of charge via the Internet at http://pubs.acs.org.

References and Notes

(1) Finlayson-Pitts, B. J.; Pitts, N. *Atmospheric Chemistry: Fundamentals and Experimental Techniques*; Wiley-Interscience; New York, 1986.

(2) Fritz, B.; Handwerk, V.; Preidel, M.; Zellner, R. *Ber. Bunsen-Ges. Phys. Chem.* **1985**, *89*, 343.

(3) Atkinson, R. J. *Phys. Chem. Ref. Data, Monograph 2* 1994.

(4) Bartolotti, L.J.; Edney, E. O. *Chem. Phys. Lett.* **1995**, *245*, 119.

(5) Vosko, S. J.; Wilk, L.; Nusair, M. *Can. J. Phys.* **1980**, *58*, 1200.

(6) Andino, J. M.; Smith, J. N.; Flagan, R. C.; Goddard, W. A., III; Seinfeld, J. H. *J. Phys. Chem.* **1996**, *100*, 10967.

(7) Becke, A. D. *J. Chem. Phys.* **1993**, *98*, 5648.

(8) García-Cruz, I.; Castro, M.; Vivier-Bunge, A. *J. Comput. Chem.* **2000**, *21*, 716.

(9) Uc, V. H.; García-Cruz, I.; Hernández-Laguna, A.; Vivier-Bunge, A. *J. Phys. Chem. A* **2000**, *104*, 7847.

(10) Uc, V. H.; García-Cruz, I.; Vivier-Bunge, A. *Advanced Problems and Complex Systems*; Quantum Systems in Chemistry and Physics Vol. 2; Kluwer Academic Publishers: Great Britain, 2000; p 241.

(11) Darnall, K. R.; Atkinson, R.; Pitts, J. N., Jr. *J. Phys. Chem.* **1979**, *83*, 1943.

(12) Traynham, J. G. *Chem. Rev.* **1979**, *79*, 323.

(13) Atkinson, R.; Carter, W. P. L.; Winer, A. M. *J. Phys. Chem.* **1983**, *87*, 1605.

(14) Shepson, P. B.; Edney, E. O.; Corse, E. W. *J. Phys. Chem.* **1984**, *88*, 4122.

(15) Jolibois, F.; Cadet, J.; Grand, A.; Subra, R.; Rega, N.; Barone, V. *J. Am. Chem. Soc.* **1998**, *120*, 186 and references therein.

(16) Frisch, M. J.; Trucks, G. W.; Schlegel, H. B.; Scuseria, B. G.; Robb, M. A.; Cheeseman, J. R.; Zakrzewski, V. G.; Montgomery, J. A.; Stratmann, R. E.; Burant, J. C.; Dapprich, S.; Millam, J. M.; Daniels, A. D.; Kudin, K. N.; Strain, M. C.; Karkas, O.; Tomasi, J.; Barone, V.; Cossi, M.; Cammi, R.; Mennucci, B.; Pomelli, C.; Adamo, C.; Clifford, S.; Ochterski, G.; Petersson, G. A.; Ayala, P. Y.; Cui, Q.; Morokuma, K.; Malick, D. K.; Rabuck, A. D.; Raghavachari, K.; Foresman, J. B.; Cioslowski, J.; Ortiz, J. V.; Stefanov, B. B.; Liu, G.; Liashenko, A.; Piskorz, P.; Komaromi, I.; Gomperts, R.; Martin, R. L.; Fox, D. J.; Keith, T. A.; Al-Laham, M. A.; Peng, C. Y.; Nanayakkara, A.; Gonzalez, V.; Challacombe, M.; Gill, P. M. W.; Johnson, B. G.; Chen, W.; Wong, M. W.; Andres, J. L.; Head-Gordon, M.; Replogle, E. S.; Pople, J. A. *Gaussian98*, revision A.1; Gaussian, Inc.: Pittsburgh, PA, 1998.

(17) Rega, N.; Cossi, M.; Barone, V. *J. Chem. Phys.* **1996**, *105*, 11060.

(18) Barone, V. *Recent Advances in Density Functional Methods*; Chong, D. P., Ed.; World Scientific Publishing: 1996; Part I, Chapter 8, p 278.

(19) Jolibois, F. Ph.D. Thesis, Université Joseph Fourier, Grenoble, France, 1997.

(20) Fujita, S.; Steenken, S. *J. Am. Chem. Soc.* **1981**, *103*, 2540. Jovanic, S. *J. Serb. Chem. Soc.* **1986**, *51*, 389.

(21) Sekušak, S.; Liedl, K. R.; Sabljić, A. J. *Phys. Chem. A* **1998**, *102*, 1583.

(22) Alvarez-Idaboy, J. R.; Mora-Diez, N.; Vivier-Bunge, A. *J. Am. Chem. Soc.* **2000**, *122*, 3715.

(23) Nicolau, C.; McMillan, M.; Norman, R. O. C. *Biochim. Biophys. Acta* **1968**, *174*, 413. Behrens, G.; Hildenbrand, R.; Shulte-Frohlinde, D.; Herak, J. N. *Perkin Trans. 2* **1988**, 305.

(24) Nicolau, C.; McMillan, M.; Norman, R. O. C. *Biochim. Biophys. Acta* **1968**, *174*, 413. Dertinger, H.; Nicolau, C. *Biochim. Biophys. Acta* **1970**, *199*, 316.